Title page

Title: Increasing Urban Tram System Efficiency, With Battery Storage and Electric Vehicle Charging

Authors:

1) Zhang, Teng

Department of Electronic and Electrical Engineering, The University of Sheffield, 3 Solly Street, Sheffield, S1 4DE, UK

Email: tzhang43@sheffield.ac.uk

2) Zhao, Rui

Department of Electronic and Electrical Engineering, The University of Sheffield, 3 Solly Street, Sheffield, S1 4DE, UK

Email: rzhao@sheffield.ac.uk

3) Ballantyne, Erica, E.F.

Sheffield University Management School, The University of Sheffield, Conduit Road, Sheffield, S10 1FL, UK

Email: e.e.ballantyne@sheffield.ac.uk

4) Stone, David. A

Department of Electronic and Electrical Engineering, The University of Sheffield, 3 Solly Street, Sheffield, S1 4DE, UK

Email: d.a.stone@sheffield.ac.uk

Corresponding author:

Ballantyne, Erica.E.F.

Email:e.e.ballantyne@sheffield.ac.uk

Keywords: Energy storage; urban trams; electric vehicle charging; electric vehicles.

Declarations of interest: none

Funding source: This work was supported by the Grantham Centre for Sustainable Futures, University of Sheffield, Sheffield, S10 2TN, UK.

Abbreviations and Acronyms

a – acceleration

C – Capacity rate for the battery

CO2e – Carbon Dioxide Equivalent

dc – Direct Current

E_{reg} – Energy regenerated by the tram

E_{res} – Energy in the dump resistor

E_{Sub} – Energy from the substation

ESS – Energy Storage Systems

E_t – Energy consumed by the tram

EV – Electric Vehicle

F_{Joint} - Sum of forces on the tram

$f_{Resistance}$ – Resistance force

F_T – Motor output force

$F_{Traction}$ – Electric motor traction force

g – force of gravity

GPS – Global Positioning System

I_e – Motor current

I_{reg} – Regenerated current

I_{res} – Dump resistor current

I_S – Current supplied from the substation

I_t – Tram current

k – Motor force constant

kg – kilogramme

km – kilometre

LatA – Latitude of point A

LonA – Longitude of point A

M_{tram} - Mass of the tram

P&R – Park and Ride

R – Radius of Earth

R2R – Road to Rail

RoI – Return on Investment

S – Distance

S – Distance

t – time

T_{grad} – Track gradient

v – speed

V – Volts

V2G – Vehicle to Grid

Vmax – maximum working voltage of a cell

V_{reg} – Tram voltage during regeneration

V_{res} – Dumo resistor voltage

V_s – Voltage at the substation

V_t – Tram Voltage

Title: Increasing Urban Tram System Efficiency, With Battery Storage and Electric Vehicle Charging

Abstract:

This paper examines the possible placement of Energy Storage Systems (ESS) on an urban tram system for the purpose of exploring potential increases in operating efficiency through the examination of different locations for battery energy storage. Further, the paper suggests the utilisation of Electric Vehicle (EV) batteries at existing Park and Ride (P&R) sites as a means of achieving additional energy storage at these locations. The study achieves this through MATLAB modelling utilising captured GPS data and publically available information. This study examines the scenario of uni-directional substations with no interconnection between the overhead catenary for both directions of travel, and discusses the trade-offs between ESS size and required current limits.

The results show the savings in both energy and basic CO_2 emissions alongside the discussion of Return on Investment (RoI) that can be achieved through the potential installation of ESS at identified ideal locations along the tram network. Moreover, this may be extended to the use of EVs as stationary ESS sited at the existing P&R facilities. Further, the model may also be used to inform future infrastructure upgrades and potential improvements to air quality within urban environments.

Keywords: Energy storage; urban trams; electric vehicle charging; electric vehicles.

1. Introduction

There is a growing interest in 'green' energy, prompted by both government regulations, and general interest amongst the population in achieving a low carbon future through the adoption of cleaner transportation (Rezvani et al., 2015; Brady and O'Mahony, 2011). Increasingly urban areas are seeing electrified transport networks such as light rail and tram systems as a viable method for reducing traffic congestion and associated transport emissions (Nichols et al., 2015; Zeng et al., 2012). These systems commonly include Park and Ride (P&R) sites to reduce passenger car vehicle movements across densely populated urban areas, particularly where there exists or is planned for the introduction of a city wide environmental policy, such as a clean air zone (Ellison et al., 2013). The purpose of this paper is to explore the concept of utilising stationary Electric Vehicle (EV) batteries in a P&R facility to act as lineside energy storage for urban dc tram systems as a method of reducing the capital expenditure required to achieve operational efficiency improvements in the tram system.

In a typical tram system, substations are generally uni-directional to save infrastructure costs, taking energy from the utility network and supplying it to the dc tram network (typically at 750V dc). The consequence of such uni-directional substations is that any energy regenerated by braking trams cannot be fed back into the utility grid. A small portion of the regenerated energy can be used by ancillary loads onboard ('Hotel loads') for heating, lighting and air-conditioning etc., however the majority of it is fed back into the tram system, where, if there is another tram accelerating in the same section of track, it can be utilised. However, if no other tram is present in the same section, the regenerated energy causes the catenary voltage to rise, potentially causing issues with the voltage rating of the tram and general infrastructure. To prevent excessive voltage rise, and to dissipate this excess energy, trams are usually equipped with a resistive dump, such that if the catenary voltage rises too high, excess energy is dissipated as heat. The downside of this feature is that it lowers overall system energy efficiency, since the regenerated energy is not usefully utilised. This issue becomes of even greater significance in an enclosed tram or metro system, such as the London Underground, where the wasted energy is dissipated as heat, thus causing the entire ambient temperature of the tunnels and stations to rise. This leads to increased air conditioning costs to return the ambient temperature to more comfortable levels for passengers at even greater expense and energy utilisation. The introduction of lineside energy storage into a network therefore alleviates these problems by giving the regenerative energy somewhere to be stored until required, without the losses associated with dumping the energy into resistors, albeit with an associated capital cost.

Taking the city of Sheffield, UK as an example, an anticipated clean air zone is expected to promote an increased use of the city's tram network; which will likely encourage greater use of the Supertram P&R sites, as well as promote and incentivise drivers to switch to EVs. This would result in an increasing number of available and stationary EVs in P&R facilities during large proportions of the working day. As EV batteries are inherently dc, there are efficiency savings to be gained from utilising the discussed regenerated energy in the dc tram system, with dc to dc conversion to the vehicles acting as additional lineside storage. This is inherently more efficient than the dc to ac current conversion that is employed in typical Vehicle to Grid (V2G) systems. This investigation focuses on the city of Sheffield, UK, where the city's tram system is typical of urban light rail / tram systems throughout the UK and worldwide, therefore the energy savings demonstrated in this paper may be extrapolated to other such systems.

The remainder of this paper discusses the application of lineside ESS on urban light rail systems, and describes the characteristics of the Sheffield tram system (Section 2); Section 3 details the energy modelling approach taken; Section 4 presents the results of the study; and Section 5 concludes the work and discusses the findings of the study.

2. Research Approach

To date, there have been a number of studies of lineside storage on urban light rail systems. Barrero et al. (2008) studied the Brussels metro line 2 which has a total length of 8 km, with 14 stops and 9 uni-directional power supply substations, and is operated with an open-circuit voltage of 876V. Teymourfar et al. (2012) studied the Tehran line-3 metro which is operated with a nominal voltage of 750V, and developed an effective method to predict the maximum instantaneous regenerative energy produced at each stop from the simulation in the 'PSCAD' circuit simulation package. The study also found that regenerative energy produced at each stop varies from 533 MWh/year to 5,900 MWh/year.

Lee et al. (2011) studied the Seoul Metro Line 7 which is composed of 42 stations and 16 substations over a 47.1 km long track, and the study uses a power flow algorithm (Lagrange optimization and gradient search iterative method) to model a railway system with ESS installed and to calculate the optimal power and capacity of the ESS required.

Various studies suggest V2G can be used for integration of renewable energy generation (Mwasilu et al., 2014, Richardson, 2013). Through the use of the 'EnergyPlan' model, Lund and Kempton (2008) found that V2G operation can absorb excess generation from wind power, and increase the overall utilization of wind power in the electricity grid. Haddadian et al. (2015) investigated using V2G to increase the penetration of different renewable resources without harming the system security and stability. Ul-Haq et al. (2017) studied an EV charging station that is either powered by photovoltaic (PV) panels, or the power grid, where V2G is used to stabilise the grid during peak load hours. The simulation results demonstrate the feasibility of the charging station under different operating modes, together with the V2G operation (Ul-Haq et al., 2017).

These studies show the installation of stationary ESS onto urban light rail systems is proven to be able to store the recovered regenerated energy, and subsequently deliver energy savings. However, to date little research has explored the potential for utilising EV batteries as ESS for light rail / urban tram systems, which forms the basis of the research presented in this paper.

The Sheffield Supertram offers an ideal opportunity for studying both the effects of lineside ESS, and the potential for EV's to act as lineside ESS, for the following reasons: the population of Sheffield is 575,424 (ONS, 2016) which is representative of a medium sized city in the UK; the city is expected to establish a clean air zone; it has an established but modern tram network that is fairly extensive, covering a total distance of 34.6km (Topp, 1999); the network has a number of established P&R systems in place; a planned network renewal and upgrade is due after 2020, with the possibility of incorporating energy storage onto the network as part of the upgrade to increase operating efficiency and lower running costs; it is a typical system in terms of current and voltage levels; the topography of Sheffield leads to high power demands, both traction and regenerative, on the trams due to the number of atypical inclines on the routes; and the Sheffield tram network is local to the authors giving easy access for data collection.

The Supertram network consists of three lines (or routes) and 48 stops. There are also 12 substations to supply energy to the system. The map of the Supertram is shown in Fig 1. The substations are located at the stops identified with a red underline in Fig 1. There are also overlaps between lines where the routes utilise the same rails, for example, as seen in Fig 1, the blue line and the yellow line overlap from 'Hillsborough' to 'Fitzalan Square', the blue line and the purple line overlap from 'Cathedral' to 'Gleadless Townend', and the yellow line and the purple line overlap from 'Cathedral' to 'Fitzalan Square'.

In order to create a model of the Supertram network to predict energy utilisation across the operating timetable, a high resolution GPS device (GARMIN eTrex® 10) was used to map the network and tram operation. The GPS measured altitude, position, and time over the sample journeys at one second intervals, these being taken over 3-days including morning and afternoon periods. From this GPS data, and the publically available mechanical characteristics of the trams, we were able to calculate the force and hence determine the energy demand of the tram. This is similar to the approach taken by Gonder et al. (2007) who utilised GPS techniques to model vehicle fleet energy consumption using GPS data in the ADVISOR program within the MATLAB environment.

To calculate and examine the energy usage of the entire network, GPS data from both operational directions of each line is required. As part of the network has tram tracks inset into the road system, the tram timings are affected by the road conditions, and this pattern varies randomly. In order to get reliable and representative data, the data collection took place on three different days during a week, in both mornings and afternoons for each route, giving 6 sets of data in total.

In detail, data was collected on Tuesday 19th, Wednesday 20th and Thursday 21st, June 2018, in the morning and afternoon. Morning data collection began on the Purple line tram journey (Fig 1) which departed at 08:20 from 'Cathedral' to 'Herdings Park'. Afternoon data collection began on the Purple line tram journey which departed at 13:45 from 'Cathedral' to 'Herdings Park'.

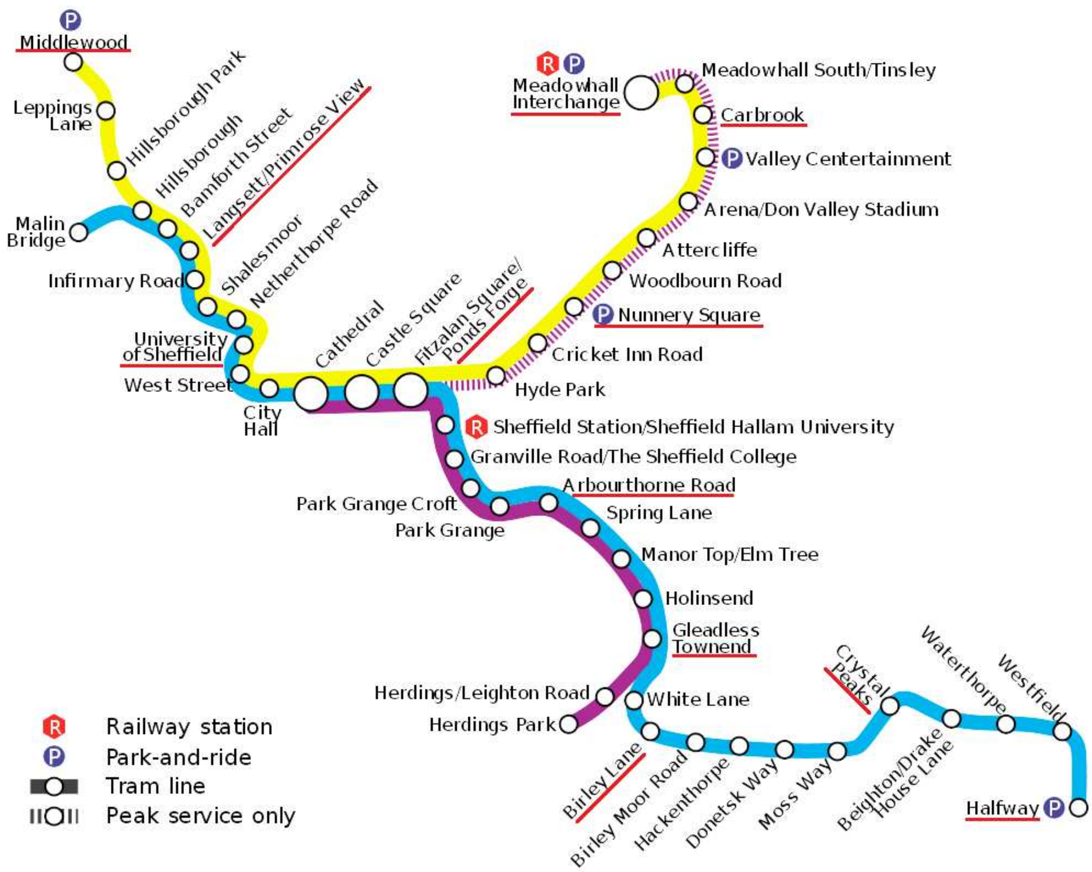

Fig. 1 The route map of the Sheffield Supertram (www.goyorkshire.com, 2018)

8 tram journeys were taken in sequence during each data collection period, Table 1.

Data sequence	Initial Tram Stop	Final Tram Stop
1	'Cathedral'	'Herdings park'
2	'Herdings Park'	'Gleadless Townend'
3	'Gleadless Townend'	'Halfway'
4	'Halfway'	'Malin Bridge'
5	'Malin Bridge'	'Langsett'
6	'Langsett'	'Middlewood'

7	‘Middlewood’	‘Meadowhall’
8	‘Meadowhall’	‘Cathedral’

Table 1 – GPS data collection journey sequence

As an example of the data collected from an individual journey, the mean height above sea level on the ‘blue route’ from ‘Halfway’ to ‘Malin Bridge’ is displayed in Fig. 2. Here, the tram stop positions are highlighted with dots within the plot.

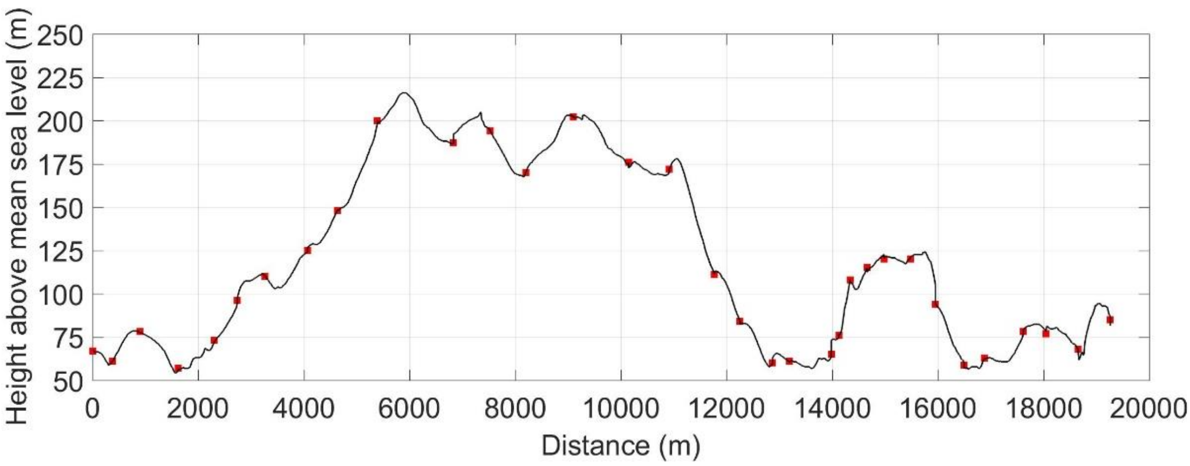

Fig. 2 The change of height above mean sea level and distance over time during the journey from ‘Halfway’ to ‘Malin Bridge’ (Dots highlight tram stop locations)

3. Energy modelling of Sheffield Supertram

3.1 Data collection and chosen modelling methodology

Raw GPS data consists of latitude and longitude coordinates. The coordinates are collected second by second, and hence, the travelling distance per second can be calculated. If the latitude and longitude of Point A are (LatA, LonA) and of Point B is (LatB, LonB), then the distance (S) between Point A and Point B is calculated via Equ 1.

$$S = R \times \arccos[\sin(LatA) \times \sin(LatB) + \cos(LatA) \times \cos(LatB) * \cos(LonA - LonB) \quad (1)$$

where *R* is the radius of the earth which is taken as 6,371,000m.

From the distance travelled per second, the speed and acceleration can be calculated via Equ 2.

$$S(t) = \int v(t)dt = \iint a(t)dt \qquad (2)$$

where S is distance, t is time, v is speed, and a is acceleration.

A typical speed trace calculated from this data is shown in Fig. 3.

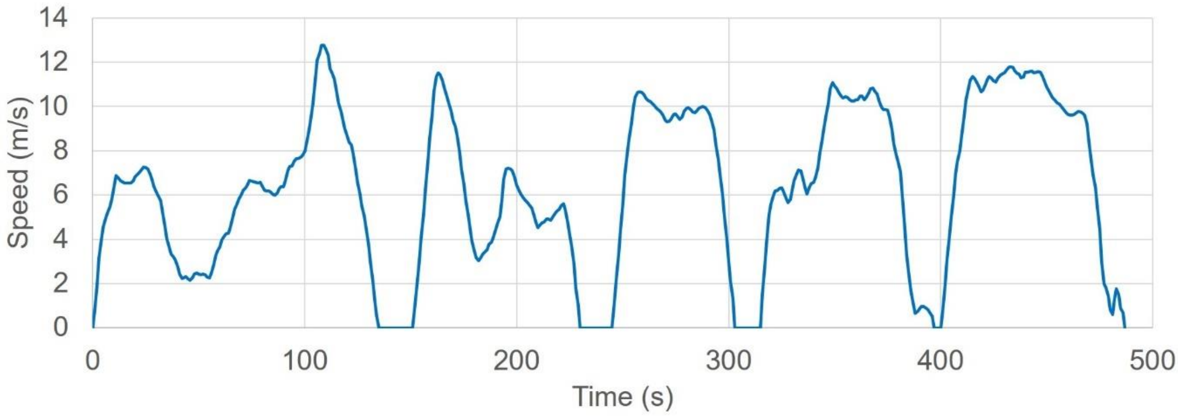

Fig. 3 The speed data collected via GARMIN eTrex® 10

From the data collected, and the mechanical parameters of the tram, forces on the tram may be simply modelled. Generally, while the tram is moving, the force that impacts the tram is the 'joint force' (F_{Joint}), consisting of the sum of the 'traction force' ($F_{Traction}$) provided by the electric motor, and 'resistance' ($f_{Resistance}$). Hence, the $F_{Traction}$ provided by the electric motor can be calculated via Equ. 3.

$$F_{Traction} = F_{Joint} - f_{Resistance} \qquad (3)$$

All three forces are vectors. As the resistance is always in the opposite direction of the movement of the tram, $f_{Resistance}$ is always negative. While the tram is accelerating, the acceleration has a positive value. Therefore, $F_{Joint\ Force}$ and $F_{Traction}$ both have positive values, and the traction force equals $F_{Traction}$. While the tram is travelling at a constant speed, $F_{Joint\ Force}$ is 0, and hence $F_{Traction}$ equals $f_{Resistance}$. While the tram is decelerating, $F_{Joint\ Force}$ is negative. From this, the electrical supply required by the tram may be calculated.

The F_{Joint} can be calculated from Equ. 4 utilising Newton's second law.

$$F_{Joint} = M_{tram} \times \mathrm{a} \tag{4}$$

where M_{tram} is the mass of the tram, obtained from public data, and a is the acceleration.

The tare weight and the passenger capacity of a single tram is 46,500 kg and 88 seats, respectively (Stagecoach, 2018). Assuming the average weight of a passenger is 60 kg (assuming a mixed demographic of men, women and children), the total mass of a tram car is estimated as 46,500+(88×60) = 51,780 kg.

In operation, the resistance force on the tram opposing its movement consists of basic resistance and additional resistance. Basic resistance comprises, motion resistance between the parts of the tram, air resistance, and is also caused by the impact and friction between the wheels and rails. There are many factors that affect the basic resistance of the tram, and some are unable to be quantified. In order to simplify the calculation of the basic resistance, the Davis equation is commonly applied to approximately express this, based on empirical data, and the type of trams. Hence, the basic resistance can be calculated via Equ. 5 (Davis, 1926; Hansen et al., 2017).

$$f_1 = \mathrm{a} + \mathrm{bv} + cv^2 \tag{5}$$

where v is the velocity, and *a, b, c* is vehicle-related experience constant. In this study, a is taken as 1.01, b is taken as 0, and c is taken as 0.0006 (Rochard and Schmid, 2000; Hansen et al., 2017). Additional resistance is caused by the road condition. The additional resistance is also calculated via Equ. 6 (Rupp et al., 2016).

$$f_2 = M_{tram} g \, sin\left[tan^{-1}\left(\frac{T_{grad}}{100}\right)\right] \tag{6}$$

where M_{tram} is the mass of the tram, g is the gravity and T_{grad} is the track gradient in percentage and is obtained from the height above mean sea level.

From Equs. (3) to (6), the traction force of the tram of any moment during the journey can therefore be calculated and forms the input into the energy trend model. As an example, the journey from ‘Halfway’ to ‘Gleadless Townend’ is used for illustration, and the calculated traction force of the tram during this journey is shown in Fig. 4.

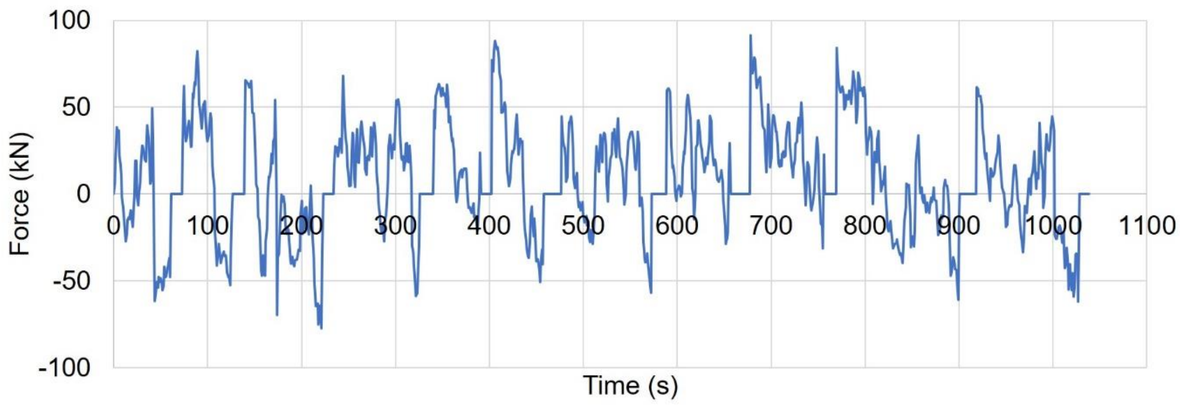

Fig. 4. The traction force of the tram of journey from Halfway to Gleadless Townend

From the force, the current drawn by the tram may be calculated. The traction motors used in the trams are the Siemens 1KB2121 and 1KB2021 (Stagecoach, 2018). Both motors are Asynchronous AC motor / drive combinations, which feature a linear relationship between the rated torque and the rated current (I_e) (Ruigang et al., 2017). Therefore, a linear relationship with the I_e and the force from the motor (F_T) is deduced and can be expressed as Equ. 7.

$$I_e = k * F_T \tag{7}$$

where k is a constant.

The force constant, k, representing not only the motor, but the whole drive-train of the tram, can be approximated to 14 under traction conditions (Du et al., 2010), and to 10 under braking (Yu et al., 2010) for systems similar to Supertram.

3.2 Model implementation

Here the methodology discussed above has been implemented in Matlab Simulink to include the whole Sheffield Supertram network. For illustration, the tram journey from Halfway to Crystal Peaks is described in detail. The implementation includes both directions of travel, city centre outbound and city centre inbound routes respectively. The corresponding Simulink schematic for the illustrative section of the network is shown in Fig. 5. As can be seen in the figure, the 'CAL P' and 'CAL N' blocks are the main calculation modules; 'Substation1' and 'Substation2' represent the substations; 'tram1' to 'tram4' are the tram modules; 'PR1' to 'PR4' and 'NR1' to 'NR4' are the line resistance modules respectively; and 'ESS' is the energy storage module for this section.

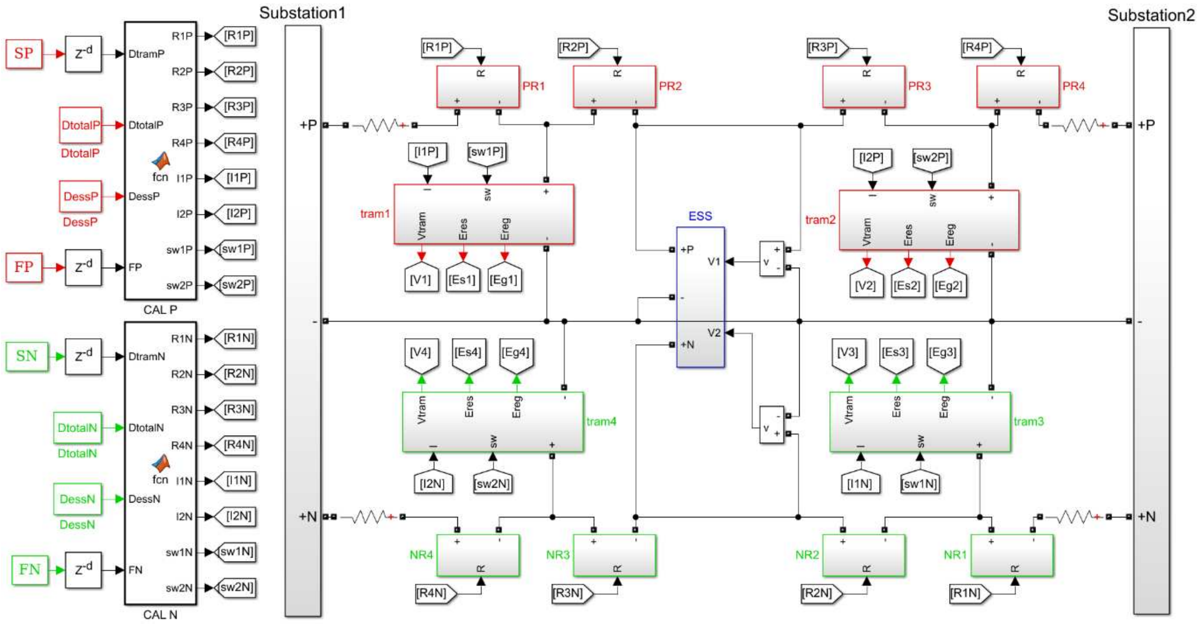

Fig. 5. Simulink model illustrating a section of the tram network model

The tramcar model is shown in Fig. 6(a). A Controlled Current Source, is used to simulate the tramcar demand on the network. Additionally, the hotel load is included to simulate the energy consumption on lighting and heating. The model also includes resistive braking, and hence the energy lost in this resistor during the tram braking is calculated.

The detailed structure of the Substation model is shown in Fig. 6(b). The substations are modelled as a Thevenin equivalent circuit, i.e. a DC voltage source and internal resistance. The DC voltage source is nominally set as 750V, with an internal resistance of 0.02Ω. The addition of the diode unit achieves the unidirectional energy supply typical of tram applications.

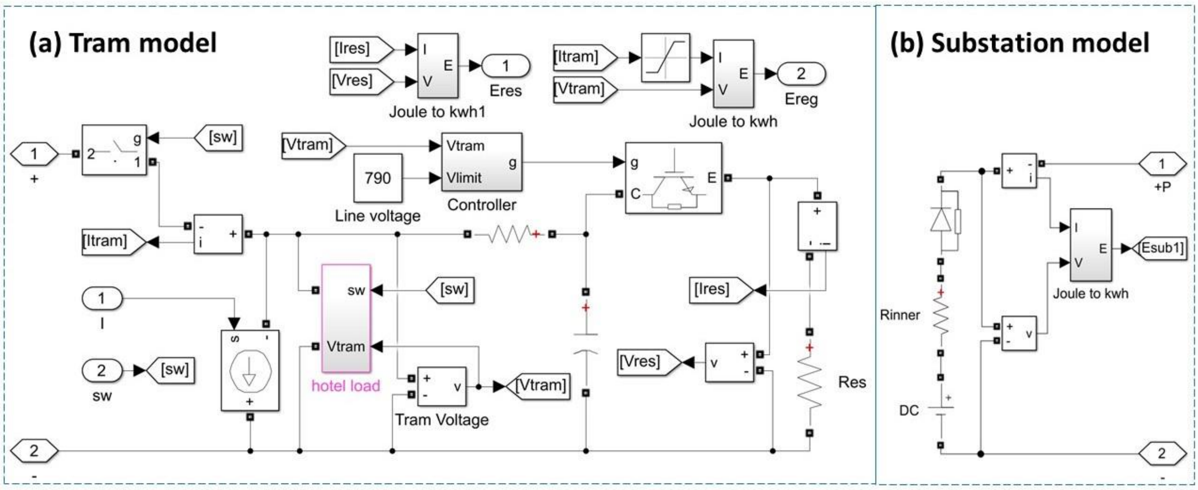

Fig. 6. Detailed models of a tramcar (a) and a substation (b)

The ESS model consists of a converter and a battery, as shown in Fig.7. The bidirectional converter comprises an IGBT based buck-boost converter. This allows controlled charge and discharge of the ESS from / to the track. The battery voltage is nominally set at 390V.

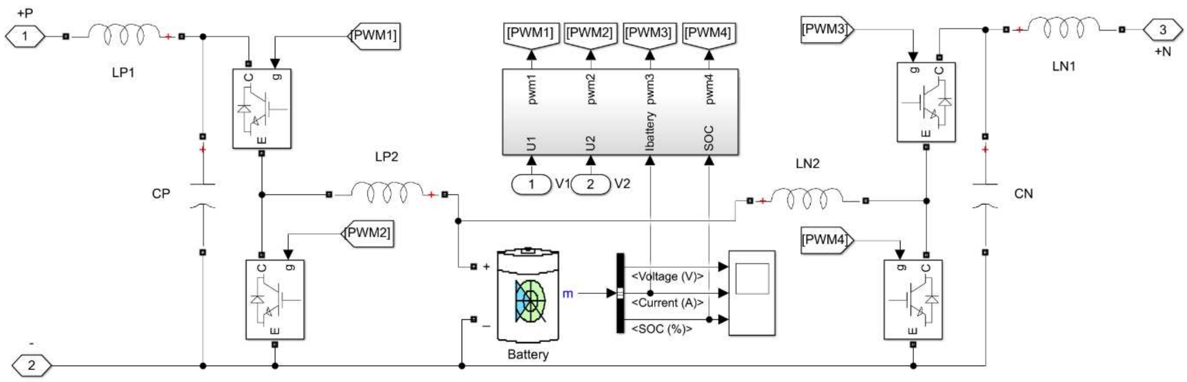

Fig. 7. The model of the ESS module

From the previously calculated tram current profile, the MATLAB model allows calculation of the voltages for the trams and substations in the whole system, which incorporates the track and catenary resistances, and electrical models of the substations. The current operating timetable for the Supertram and the logged data for the sample journeys and are used as model inputs to simulate the tram movements. Therefore, the energy utilised from the substation (E_{Sub}), electricity consumed in the dump / braking resistor (E_{res}), electricity consumed by the tram (E_t) and regenerative energy (E_{reg}) can be calculated via Equs. (8) to (11) respectively.

$$\boldsymbol{E_{sub} = \int I_{sub} \cdot V_{sub} d_t} \tag{8}$$

Where I_{sub} is the current drawn from the substation, and V_{sub} is the voltage at the given substation

$$\boldsymbol{E_{res} = \int I_{res} \cdot V_{res} d_t} \tag{9}$$

Where I_{res} is the current and V_{res} is the voltage of across the dump resistor.

$$\boldsymbol{E_t = \int I_t \cdot V_t d_t} \tag{10}$$

Where I_t is the current from the catenary to the tram and V_t is the voltage at the tram.

$$\boldsymbol{E_{reg} = \int I_{reg} \cdot V_{reg} d_t} \tag{11}$$

Where I_{reg} is the current from the tram to the catenary, and V_{reg} is the voltage of the tram.

From the models, the daily energy balance across the network, considering E_{sub}, E_{res} and E_{reg}, can be obtained and is shown in Fig 8. Based on the journey data collected on different dates and times, the energy trends appear to show little variation with traffic conditions and passenger numbers, as the passenger numbers and traffic conditions will not be the same for each journey. Typically, the morning data samples were taken close to the 'rush hour' period, and the afternoon samples were under lighter traffic and passenger number conditions. Thus the energy used from the substations on the network are within +/- 2% of the average across the 6 sampled journey sets. This approach to the daily energy utilisation calculations appears to be an acceptable approximation, based on the consistency of the results shown, and therefore forms a useful base on which to examine the integration of EV's into the tram network as part of the proposed ESS.

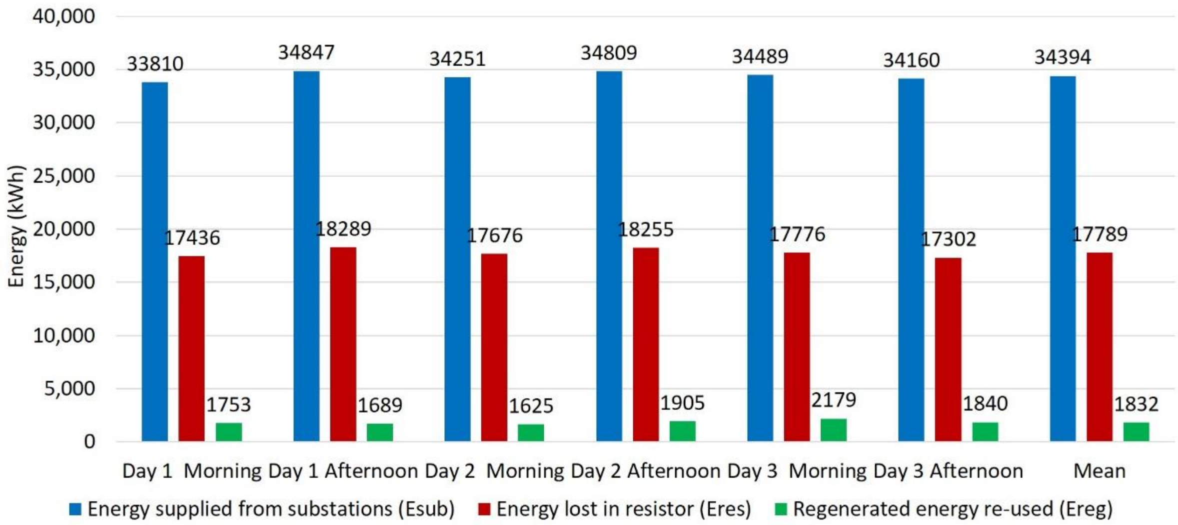

Fig. 8. Calculated Daily Energy trends using data captured on morning and afternoon of 19th to 21st June 2018.

4. Results and Discussion

Using the model, it is possible to determine a maximum size of ESS required to achieve sensible system operation. From the model, the maximum current drawn by the tram was calculated as less than 1,300A at peak traction force. For example, using the tram journey from Halfway to Gleadless Townend for illustration (as shown in Fig. 9), the traction current remains within 1,000A for the majority of the journey, rarely going above 1,000A or reaching the maximum value of 1,300A. Given the nature of the converters within the ESS model, the maximum practical current likely to be seen by the battery is therefore limited to around 2,000A.

This allows ESS selection to be based on the current rating of the batteries used. Normally, a battery operating current can be quoted in terms of its capacity. For example, a 100Ah battery can be expected to supply 100A for 1 hour, termed the 'C' rate, and 100A drawn from the example battery is referred to as 1C. Similarly, if 50A is drawn from the battery, it should supply the current for 2 hours, termed 0.5C or C/2. 200A is similarly termed the 2C rate for the example battery. This then allows comparison between the operating characteristics of battery packs of different capacities. Normally, lithium-based batteries are limited to a maximum rate of 2C to prevent damage to the cells in the battery packs.

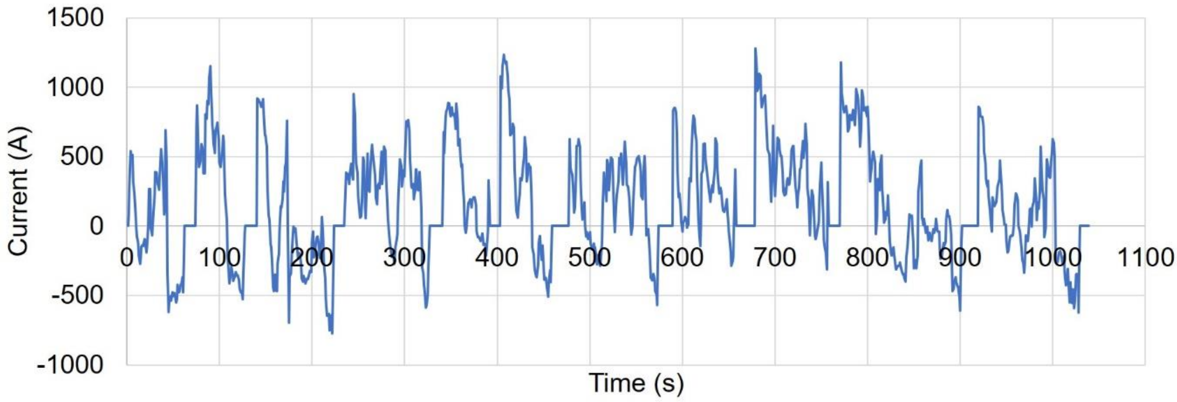

Fig.9. The profile of traction current of tram journey from Halfway to Gleadless Townend

As the maximum current seen by the battery is 2000A, and we wish to limit the battery current to 2C, the initial study is carried out with a 1000Ah battery pack. Examining a single journey from ‘Halfway’ to ‘Crystal Peaks’ on the Blue route (Fig. 1) and placing a 1000Ah ESS at each stop in turn, results in the energy usage per journey shown in Table 2 and Fig 10.

Location of ESS	Scenario Number	Energy drawn from Halfway substation (kwh)	Energy lost in resistor (kwh)	Energy drawn from Crystal Peaks substation (kwh)	Total energy from substations (kwh)
without ESS	1	7.457	7.954	6.997	14.454
Halfway	2	6.921	3.375	6.969	13.89
Westfield	3	4.759	2.451	6.146	10.905
Waterthorpe	4	5.142	1.975	5.456	10.598
Beighton	5	6.413	2.157	4.783	11.196
Crystal Peak	6	7.448	3.914	6.775	14.223

Table 2 – Energy usage for a single journey from ‘Halfway’ to ‘Crystal Peaks’ with 6 scenarios for ESS placement

From Fig 10 and Table 2, it can be seen that the least energy is drawn from the utility supply for the single journey in Scenario 4, with the ESS being placed at 'Waterthorpe' tram stop (location 4), which is between the two substations on this track section. Initially, ESS placement has been constrained to tram stop locations, as these allow easy track access and would be possible places for EV parking in future study scenarios. In the best scenario, the energy lost in the braking resistors is reduced from 9.580kWh to 2.939kWh per journey, a reduction in loss of 69%. The energy drawn from the utility supply for this single journey is also reduced from 16.831kWh to 12.031kWh, equating to a reduction of ~29%, due to the re-cycling of the captured energy from tram braking, used in subsequent accelerations. This therefore points towards the optimum location for ESS, located at existing tram stops, to be as close as possible to the mid-point between any two substations.

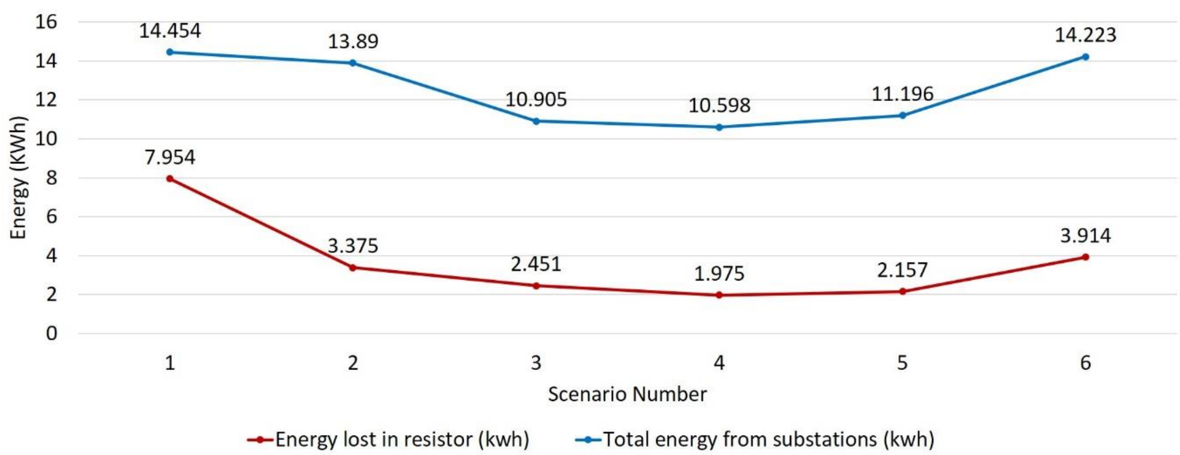

Fig. 10. Energy use for a single journey from 'Halfway' to 'Crystal Peaks' with 6 scenarios for the ESS placement

Utilising this ESS position, Table 3 shows the effect of using a smaller ESS (200Ah), and applying different current limits to the operation, from 0.5C to 10C, given that the upper value is commensurate with the 1000Ah, 2C scenario above. Whilst this high current rate may not be practical at this time, future developments may not prevent operation at this rate. Plotting these in Fig 11 shows a trend of diminishing returns, with little improvement in energy saving operating the 200Ah battery above 4C. This is true as it may be seen that the tram current rarely exceeds 4C (800A) while travelling between these substations, as shown by the simulated battery current trace, Fig 12.

Limit discharge rate (C)	Max current (A)	Energy drawn from Halfway substation (kwh)	Energy lost in resistor (kwh)	Energy drawn from Crystal Peaks substation (kwh)	Total energy from substations (kwh)
0.5	100	6.65	5.899	6.451	13.101
1	200	6.306	4.727	6.227	12.533
2	400	5.788	3.091	5.884	11.672
4	800	5.301	1.98	5.561	10.862
10	2000	5.14	1.971	5.454	10.594

Table 3 – Energy usage for a single journey from ‘Halfway’ to ‘Crystal Peaks’ with maximum current ratings from 0.5C to 10C, for a 200Ah battery at the ‘Waterthorpe’ tram stop.

Therefore, the current limit of 4C imposed on the battery is high enough to capture almost all of the energy regenerated from the trams on deceleration and return most of what is possible to the tram on acceleration. The sizing and current rating of the ESS has implications of cost and return on investment (RoI) if a purpose built ESS is to be installed.

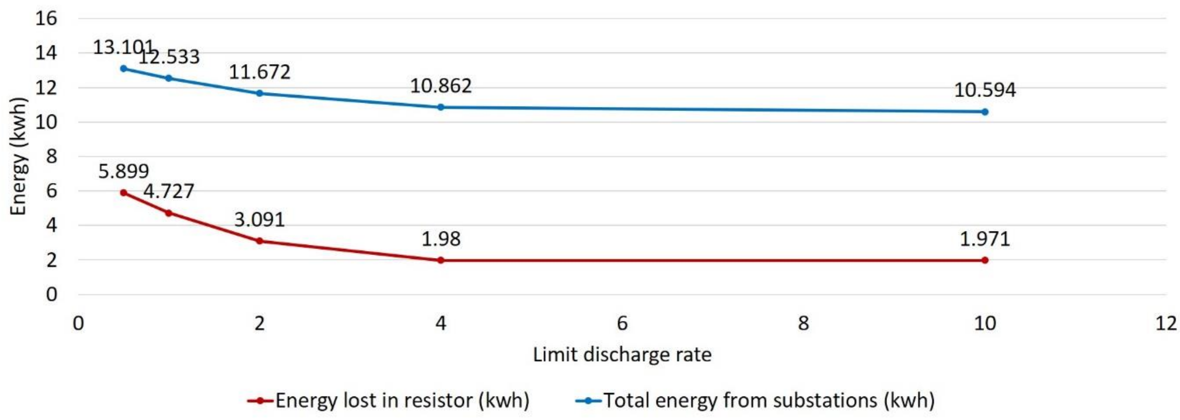

Fig. 11. Energy use for a single journey from ‘Halfway’ to ‘Crystal Peaks’ with 5 current limits for a 200Ah battery at the ‘Waterthorpe’ tram stop.

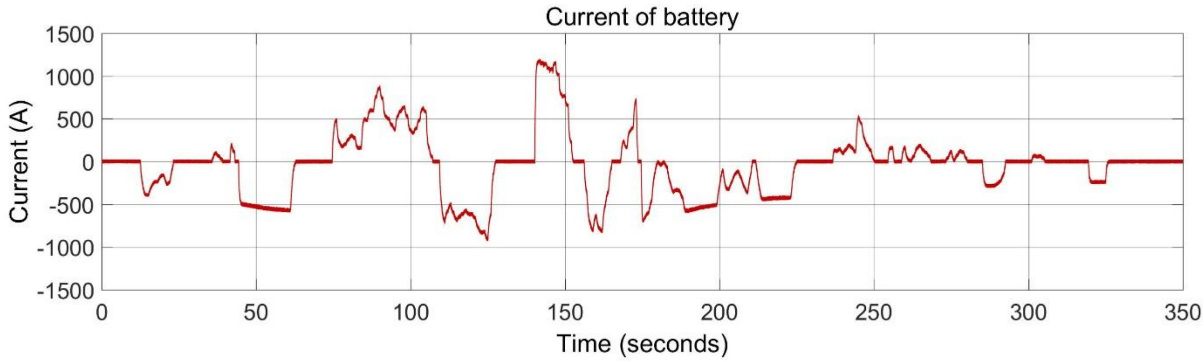

Fig. 12. Simulated battery current for a single journey from 'Halfway' to 'Crystal Peaks' with a 10C current limit applied to a 200Ah ESS at the 'Waterthorpe' tram stop.

If the ESS is only to be installed at existing P&R tram stop locations, ('Halfway', 'Middlewood', 'Meadowhall', 'Valley Centertainment' and 'Nunnery Square'), then the P&R locations are not what has been shown to be ideal, as they are coincident with, or close to, existing substations. A study of the 1000Ah ESS, limited to 2C current ratings, installed at each of the P&R locations above leads to the reduction in daily energy use of the overall tram system as shown in Fig. 13. This can be directly compared with Fig. 8.

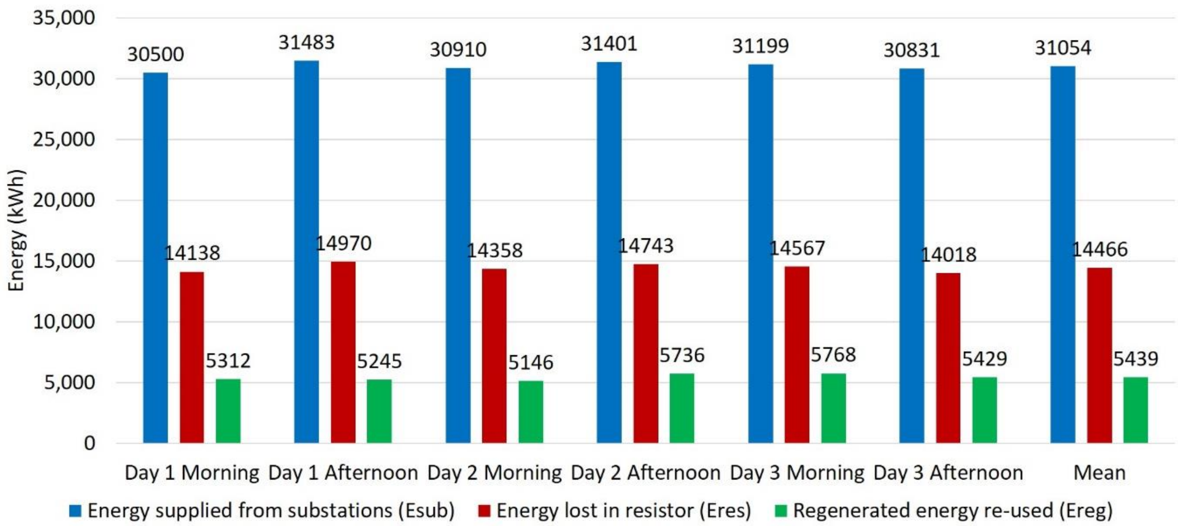

Fig. 13. Simulated Daily Energy trends with the 1000Ah ESS installed at each park and ride location on the tram network.

Whilst the existing P&R locations are not ideal, there are still energy savings to be made. The average daily energy consumption across the network falls from 34.4MWh, to 31.0MWh, a saving of 3.4MWh per day, or taking operation over 364 days of a year, 1237.6MWh. At a typical cost per MWh of electricity in the UK of £53/MWh, this equates to a saving of £65.6k p.a. Methods of converting this electricity saving to Co2e savings vary dependant on the approach taken, but indicatively, utilising the year average from the UK Gridwatch (http://gridwatch.co.uk/co2-emissions, 2019), this gives an average Co2e emission of 9.7kiloTonnes / GWh of energy generated on the UK grid. This therefore equates the 1237.8MWh electricity saving to a saving of 12.0kilo tonnes CO2e.

A 1000Ah battery, at 390V nominal, results in an ESS capacity of 0.39MWh. If this is to be a purpose built ESS, then the RoI can be calculated. Typically, a 0.39MWh Lithium based battery can be supplied, fully installed for grid support at ~£150k, giving a RoI for 5 such systems, installed at the P&R locations (shown in Fig. 1) as ~11.4 years based on energy savings alone, which may be seen as an unacceptably long period of time, both in terms of investment, and lifetime of the batteries.

However, a single Nissan Leaf EV has a battery capacity of 40-62kWh dependant on the model (Nissan, 2019). Taking an average of 50kWh, the P&R scenario requires ~8 x Nissan Leaf EV's to be parked at each P&R site to achieve this required ESS capacity. Larger EV's, for example the TESLA, have a battery capacity of up to 100kWh (Tesla, 2019), thus requiring fewer vehicles to be available for ESS use.

One possible technical argument against this idea of the EV batteries being used by the tram system, and against V2G in general, is the consequent cycling of the EV batteries and loss of capacity. If the single journey from 'Halfway' to 'Crystal Peaks' is taken as an example, using data from Table 2, it is possible to calculate the energy going into the ESS as the difference between the energy lost in the tram braking resistors in scenarios 1 and 2, that is, without an ESS, and with an ESS installed at the 'Halfway' tram stop. In this case the energy difference is 0.56kWh. With a 390kWh ESS installed at 'Halfway', the state of charge (SoC) of the ESS would only change by 0.14% for each journey, as the battery sizing requirement is power driven to limit the battery current, and not energy driven in this case. This very small change in SoC would not give rise to significant cycling of any ESS at this location, with negligible subsequent effect on battery lifetime (Millner, 2010).

A further advantage may be obtained from the fact that the tram only operates from 'Halfway' every 10 minutes, therefore the 'Halfway' substation could be utilised to charge EVs connected to the supply between scheduled trams, without the need for the supplementary grid reinforcement normally required to install a number of EV chargers at a given location. Given the scenario whereby the EV's are parked at the P&R facility for most of the working day, the integration of the road and tram system could result in benefits for both the tram network, and the vehicle owners with reduced charging costs for allowing their vehicles to participate in an additional lineside energy storage system.

To complete the study of ESS utilisation, in a different scenario, the 1000Ah ESS could be added to the network at the 'ideal' locations as discussed previously (at a tram stop mid-point between two substations), and this would result in the overall daily energy trends shown in Fig. 14.

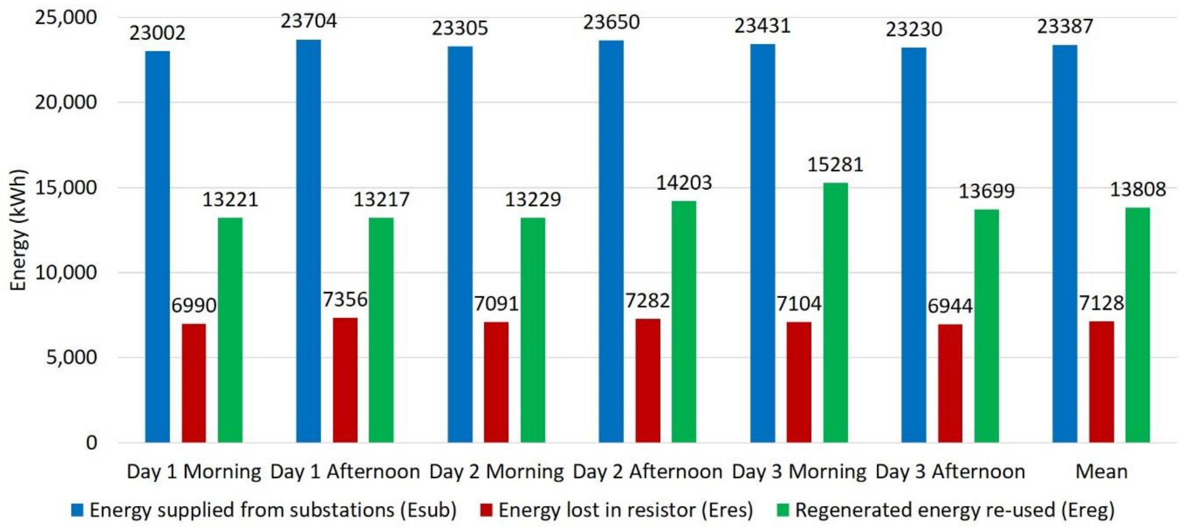

Fig. 14. Simulated Daily Energy trends with a 1000Ah ESS installed at ideal tram stop locations on the tram network.

In this case, the yearly savings on energy costs amount to ~£212k per year. (4GWh p.a.) and the yearly CO_2e savings amount to 38.96 kilo tonnes CO_2e. Here, significantly more energy is captured by the ESS and re-used within the system. However, this comes at a cost in terms of capital costs and installation / running costs of the ESS's. From Fig 1, it may be seen that 11 ESS would be required to achieve this saving. At an installation cost of £150k per ESS, the RoI would result in the payback period being ~8 years. This is still too long for investment with a battery of this size.

Reducing the battery size to 200Ah (nominally 78kWh), and limiting the operating current to 4C would, from Figure 15, capture most of the available energy at reduced ESS cost.

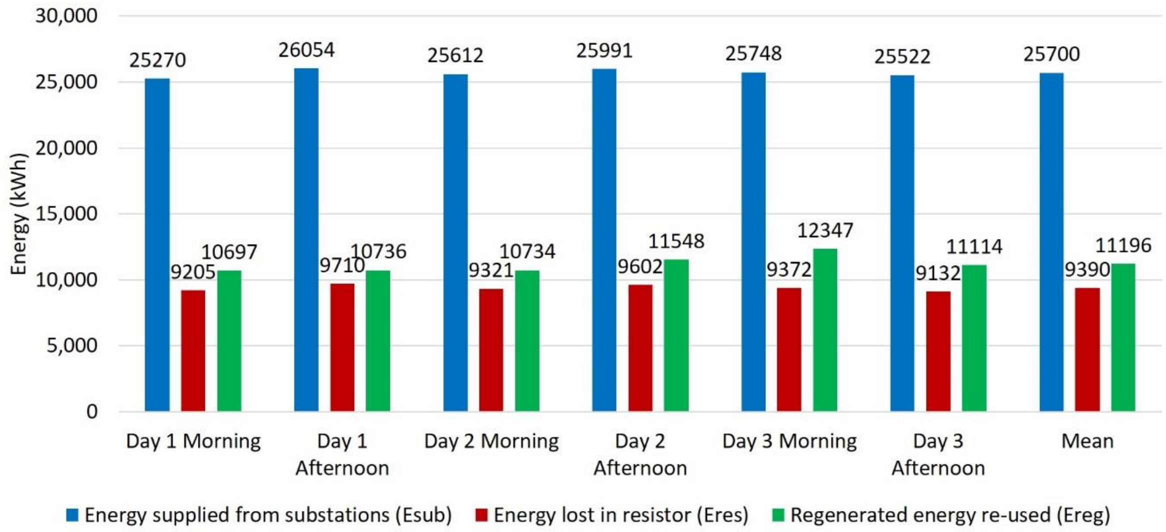

Fig. 15. Simulated Daily Energy trends with a 200Ah ESS installed at ideal tram stop locations on the tram network.

In this case, the yearly savings on energy costs amount to ~£167k per year. (3.1GWh p.a) and the yearly CO_2e savings amount to 30 kilo tonnes. Once again, 11 ESS would be required to achieve this saving. At an installation cost of £40k per ESS, the RoI would result in the payback period being ~2.6 years. This is much more attractive to implement, and easily falls within typical warranty lifetimes for ESS of ~10-15 years. Given the low change in ESS SoC per event, the 200Ah ESS, would be able to handle the 4C current rate for the short periods of time required. Additionally, the large amount of energy storage available on the system if this was installed would allow periods of tram operation independent of the grid, for example to participate in demand side response on the utility grid, or avoid peak time electricity charges, further reducing the payback time of the system. Further, the use of EV batteries in parallel with the installed ESS would further reduce the losses whilst providing the opportunity to provide vehicle charging from the tram dc supply when a tram is not in the track sections, forming an additional revenue stream.

The results of this study could therefore be used to inform siting of possible future P&R facilities, and whilst it will not be possible to provide such facilities at each 'ideal' location on the tram network for optimal energy savings, this does provide insight into the savings which could be made in operating costs. Although, any such savings in operating costs would need to be accounted for with regards to the RoI once the capital outlay of the installations has been calculated.

5. Conclusions

This paper has examined the possible placement of ESS on the Sheffield Supertram network for the purpose of exploring savings made to the operating costs of the system, and carbon emission reductions. Also, potential EV charging locations that could provide a suitable benefit for the proposed additional energy storage scheme have been discussed. This has been achieved through the use of MATLAB modelling utilising captured GPS data and publically available information. This study has examined the scenario of uni-directional substations with no interconnection between the overhead catenary for both directions of travel. Further work is on-going to examine different scenarios for system operation, and to examine the trade-offs between ESS size and required C-rate operation.

The results show that savings can be made by installation of ESS within the network, and these extend to the use of EVs as stationary ESS sited at the existing P&R facilities. The model may also be used to inform future infrastructure upgrades, and possible impact of ESS / P&R placement in future scenarios.

This study highlights the synergies which can be obtained through the integration of road and urban light rail transport systems. Whilst the study has highlighted the case of the Sheffield city region, it is highly applicable to any city or urban area where a light rail system is available or is being considered. The growing concerns around urban air quality that are leading to the widespread introduction of clean air zones in urban areas throughout the world, provoke increased uptake of electric vehicles. This increase in EV’s and growing interest in green technologies prompts the consideration of novel approaches to urban transport issues. For example, it could be envisaged that large numbers of EVs will be used as inter-urban transportation, to be parked on the outskirts of urban centres facilitating the feasibility of their use as additional energy storage on the urban tram system.

References:

BARRERO, R., TACKOEN, X., and MIERLO, J. V. 2008. Improving energy efficiency in public transport: Stationary supercapacitor based Energy Storage Systems for a metro network, in *2008 IEEE Vehicle Power and Propulsion Conference*, 3-5 Sept. 2008, pp. 1-8, doi:10.1109/VPPC.2008.4677491.

BRADY, J., and O’MAHONY, M. 2011. Travel to work in Dublin. The potential impacts of electric vehicles on climate change and urban air quality. *Transportation Research Part D, Vol. 16 pp188-193*

DAVIS, W. J. 1926. The tractive resistance of electric locomotives and cars. General Electric.

DU, F., HE, J., YU, L., LI, M., BO, Z., and KLIMEK, A. 2010. Modeling and Simulation of Metro DC Traction System with Different Motor Driven Trains, in *Power and Energy Engineering Conference (APPEEC), 2010 Asia-Pacific*, 2010: IEEE, pp. 1-4.

ELLISON, R. B., GREAVES, S. P. and HENSHER, D.A. 2013. Five years of London’s low emission zone: Effects on vehicle fleet composition and air quality. Transportation Research Part D, Vol.23 pp.25–33.

GONDER, J.; MARKEL, T.; THORNTON, M.; and SIMPSON, A. 2007. Using global positioning system travel data to assess real-world energy use of plug-in hybrid electric vehicles. Transportation Research Record: Journal of the Transportation Research Board, No. 2017, Transportation Research Board of the National Academies, Washington, D.C., 2007, pp. 26–32. DOI: 10.3141/2017-04

GRIDWATCH. 2019. C02-emissions [online] GRIDWATCH. [viewed 19 July 2019]. Available from: http://gridwatch.co.uk/c02-emissions.

GOYORKSHIRE. 2018. Stagecoach-Supertram [online]. Go Yorkshire. [Viewed 20 September 2018]. Available from: http://www.goyorkshire.com/what-to-do/activities-tours/stagecoach-supertram.

HADDADIAN, G., KHALILI, N., KHODAYAR, M. and SHAHIEDEHPOUR, M. 2015. Security-constrained power generation scheduling with thermal generating units, variable energy resources, and electric vehicle storage for V2G deployment. International Journal of Electrical Power and Energy Systems, 73, 498-507.

HANSEN, H.S., NAWAZ, M.U. and OLSSON, N., 2017. Using operational data to estimate the running resistance of trains. Estimation of the resistance in a set of Norwegian tunnels. Journal of Rail Transport Planning & Management, 7(1-2), pp.62-76.
LEE, H., SONG, J., LEE, H., LEE, C., JANG, G., and KIM, G. 2011. Capacity optimization of the supercapacitor energy storages on DC railway system using a railway powerflow algorithm, *IJICIC,* vol. 7, no. 5, pp. 2739-2753.
LUND, H. & KEMPTON, W. 2008. Integration of renewable energy into the transport and electricity sectors through V2G. Energy Policy, 36, pp. 3578-3587.
MILLNER, A. 2010. Modeling Lithium Ion battery degradation in electric vehicles. IEEE Conference on Innovative Technologies for an Efficient and Reliable Electricity Supply, September 2010, pp.349-356.
MWASILU, F., JUSTO, J. J., KIM, E. K., DO, T. D. and JUNG, J. W. 2014. Electric vehicles and smart grid interaction: A review on vehicle to grid and renewable energy sources integration. Renewable and Sustainable Energy Reviews, 34, pp. 501-516.
NICHOLS, B.G., KOCKELMAN, K.M. and REITER, M. 2015. Air quality impacts of electric vehicle adoption in Texas, Transportation Research Part D, Vol. 34, pp.208–218.
NISSAN. 2016. Prices & Specifications - Nissan LEAF - Electric Car [online]. Nissan. [Viewed 31 July 2019]. Available from: https://www.nissan.co.uk/vehicles/new-vehicles/leaf/prices-specifications.html#grade-LEAFZE1A-0
ONS. 2016. Sheffield Factsheet version 1, 2016 Mid-Year Population Estimate (ONS), Crown Copyright.
REZVANI, Z., JANSSON, J., and BODIN, J. 2015 Advances in consumer electric vehicle adoption research: A review and research agenda. Transportation Research Part D. Vol. 34. Pp122-136.
RICHARDSON, D. B. 2013. Electric vehicles and the electric grid: A review of modeling approaches, Impacts, and renewable energy integration. Renewable and Sustainable Energy Reviews, 19, pp. 247-254.
ROCHARD B. P. and SCHMID, F. 2000. A review of methods to measure and calculate train resistances, Proceedings of the Institution of Mechanical Engineers, Part F: Journal of Rail and Rapid Transit, vol. 214, no. 4, pp. 185-199.
RUIGANG, S., TIANCHEN, Y., JIAN, Y., and HAO, H. 2017. Simulation of braking energy recovery for the metro vehicles based on the traction experiment system, *Simulation,* vol. 93, no. 12, pp. 1099-1112, 2017, doi: 10.1177/0037549717726146.
RUPP, A., BAIER, H., MERTINY, P., and SECANELL, M. 2016. Analysis of a flywheel energy storage system for light rail transit, Energy, vol. 107, pp. 625-638. doi: 10.1016/j.energy.2016.04.051.
STAGECOACH. 2018. Vehicle Information.[online]. Stagecoach. [Viewed 1 November 2018]. Available from: https://www.stagecoachbus.com/supertram/vehicle-information.
TESLA. 2019. Model X Owner's Manual. [online]. Tesla. [Viewed 31 July 2019]. Available from: https://www.tesla.com/en_GB/modelx
TEYMOURFAR, R., ASAEI, B., IMAN-EINI, H., and NEJATI FARD, R. 2012. Stationary super-capacitor energy storage system to save regenerative braking energy in a metro line, *Energy Conversion and Management,* vol. 56, pp. 206-214, doi: 10.1016/j.enconman.2011.11.019.

TOPP, H.H. 1999. Innovations in tram and light rail systems, Proceedings of the Institute of Mechanical Engineers Part F, Vol.213, pp.133-141.

UL-HAQ, A., CECATI, C. and AL-AMMAR, E. A. 2017. Modeling of a photovoltaic-powered electric vehicle charging station with vehicle-to-grid implementation. Energies, 10.

YU, L., HE, J., YIP, H., DU, F., BO, Z. and HU, J. 2010. Simulation of regenerative braking in DC railway system based on MATLAB/Simulink, in *Universities Power Engineering Conference (UPEC), 2010 45th International*, 2010: IEEE, pp. 1-5.

ZENG, A.Z.; DURACH, C.F. and FANG, Y. 2012. Collaboration decisions on disruption recovery service in urban public tram systems, Transportation Research Part E, Vol. 48 pp.578–590.